



Published in final edited form as:

Ear Hear. 2016 ; 37(5): e322–e335. doi:10.1097/AUD.0000000000000324.

Human Envelope Following Responses to Amplitude Modulation: Effects of Aging and Modulation Depth

Andrew Dimitrijevic, Jamal Alsamri, M. Sasha John, David Purcell, Sahara George, and Fan-Gang Zeng

Abstract

OBJECTIVE—To record Envelope Following Responses (EFRs) to monaural amplitude-modulated broadband noise carriers in which amplitude modulation (AM) depth was slowly changed over time and to compare these objective electrophysiological measures to subjective behavioral thresholds in young normal hearing and older subjects.

DESIGN—Participants: three groups of subjects included a young normal hearing group (“YNH”, 18 to 28 years; pure tone average=9 dB HL), a first older group (“O1”; 41 to 62 years; pure tone average=30 dB HL) and a second older group (“O2”; 67 to 82 years; pure tone average=49 dB HL). Electrophysiology: In condition 1, the AM depth (41 Hz) of a white noise carrier, presented at a suprathreshold intensity of 60 dB SL, was continuously varied from 2% to 100% (5%/sec). EFRs were analyzed as a function of the AM depth. In condition 2, auditory steady-state responses (ASSRs) were recorded to fixed AM depths (100, 75, 50, and 25%) also presented at 60 dB SL with an AM rate of 41 Hz. Psychophysics: A three alternative, forced-choice procedure was used to track the amplitude modulation (AM) depth needed to detect AM at 41 Hz (AM detection). The minimum AM depth capable of eliciting a statistically detectable EFR was defined as the physiological AM detection threshold.

RESULTS—Across all ages, the fixed AM depth ASSR and swept AM EFR yielded similar response amplitudes. Statistically significant correlations ($r=0.48$) were observed between behavioral and physiological AM detection thresholds. Older subjects had slightly higher, but non-significant behavioral AM detection thresholds than younger subjects. AM detection thresholds did not correlate with age. All groups showed a sigmoidal EFR amplitude vs. AM depth function but the shape of the function differed across groups. The O2 group reached EFR amplitude plateau levels at lower modulation depths than the NH group and had a narrower neural dynamic range. In the YNH group, the EFR phase did not differ with AM depth whereas in the older group, EFR phase showed a consistent decrease with increasing AM depth. The degree of phase change (or phase-slope) was significantly correlated to the pure tone threshold at 4 kHz.

CONCLUSIONS—EFRs can be recorded using either the swept modulation depth or the discrete AM depth techniques. Sweep recordings may provide additional valuable information at suprathreshold intensities including the plateau level, slope and dynamic range. Older subjects had

Corresponding Author: Andrew Dimitrijevic, PhD, Communication Sciences Research Center, Cincinnati Children’s Hospital Medical Center, 3333 Burnet Avenue, Cincinnati, Ohio 45229-3039, andrew.dimitrijevic@cchmc.org, Phone: (513) 636-3469.

AUTHOR CONTRIBUTION STATEMENT

AD, SMJ, DP, FG, and JA designed the experiments and wrote the paper; JA and SG performed the experiments.

a reduced neural dynamic range compared to younger subjects suggesting that aging affects the ability of the auditory system to encode subtle differences in the depth of amplitude modulation. The phase-slope differences are likely related to differences in low and high frequency contributions to EFR. The behavioral-physiological AM depth threshold relationship was significant but likely too weak to be clinically useful in the present individual subjects who did not suffer from apparent temporal processing deficits.

INTRODUCTION

Temporal processing of sound is a crucial aspect in many areas of audition including sound detection, localization, and identification. Much of the information required to understand spoken language comes from the temporal envelope of speech as evidenced by our ability to understand speech with limited spectral cues (Fu, 2002; Shannon et al. 1995). Insights into the importance of temporal processing for speech are also seen with disorders arising from auditory temporal processing difficulties, such as auditory neuropathy (Starr et al., 1996) resulting in impaired speech perception (Zeng & Liu 2006). In older individuals, reduced temporal processing ability is thought to contribute to deficits in speech perception especially in noise (Anderson et al., 2012). The reduction in temporal processing in the elderly is in part associated with reductions in inhibitory neurotransmitter at various levels of the ascending auditory system including the brainstem (Wang et al. 2009), thalamus (Richardson et al., 2013) and auditory cortex (Casparly et al., 2013). This altered balance of inhibition may also be related to a reduction in neural synchrony that is normally required for precise speech encoding. Modeling auditory aging as temporal disruptions through neural jitter provides evidence that reduced temporal processing, as opposed to reduced spectral processing, is more related to reductions in speech perception in the elderly (Pichora-Fuller et al., 2007).

One commonly used method of assessing temporal processing is the temporal modulation transfer function (TMTF). The TMTF is obtained by determining the behavioral threshold for minimum modulation needed to detect amplitude modulation (AM) as a function of modulation rate. The TMTF typically has a low-pass filter shape such that AM detection threshold changes little across low frequencies (~2 to ~50 Hz). Beyond that range the AM detection threshold increases significantly, resulting in a low-pass filter characteristic (Viemeister, 1979). Behavioral measures of TMTFs in the elderly have shown overall similar shapes to young normal-hearing listeners. Elderly listeners (above 70 years) showed slightly elevated AM detection thresholds, especially for AM rates above 30 Hz (Takahashi et al. 1992). Therefore we hypothesized that in this study, a relatively small, but detectable, difference in behavioral TMTFs would be observed between young and elderly listeners.

The use of auditory evoked potentials to examine temporal processing has been the topic of a recent review by Picton (2013). In that review, it was noted that temporal resolution is often assessed using AM stimuli to evoke brain responses, by gap detection, or by recognition of single versus double stimuli. In this report, we will focus on the brain's response to AM stimuli, which are often referred to as Auditory Steady-State Responses (ASSRs). By definition, ASSRs have a stable amplitude and phase across time because the evoking stimulus (e.g., AM) is constant. However, in cases where the evoking stimulus

changes over time, as is the case for speech stimuli (Aiken & Picton 2008) or changing AM (Purcell et al. 2004), the brain response also changes. These responses are often termed Envelope Following Responses (EFRs). In effect, an ASSR is a subclass of EFRs. We recorded both ASSRs (to fixed AM depths) and EFRs (to changing AM depth), but these terms may be used here interchangeably, in accordance with the terms used by prior studies.

A number of ASSR and EFR studies have examined the temporal processing ability of the auditory system in young normal hearing and elderly participants. Purcell et al., (2004) described an EFR method of assessing temporal processing by presenting an AM stimulus that varied in modulation rate as a function of time. The brainstem EFR (modulation rates above 70 Hz AM) was significantly correlated to behavioral measures of gap and AM detection. Ross et al. (2000) examined ASSRs to a wide variety of AM rates (10 to 98 Hz) and found that the shape of the ASSR amplitude versus AM rate function resembled a psychophysically-derived TMTF. In a study that examined ASSRs and aging, Boettcher et al., (2001) recorded ASSRs to stimuli with high and low frequency pure tone carriers at an AM rate of 40 Hz with various AM depths. In the elderly with high frequency hearing loss, ASSRs to a low frequency carrier were reduced compared to normal hearing (NH) controls. Further, this was not found in older subjects with no high frequency hearing loss. Along similar lines, Leigh-Paffenroth & Fowler (2006) examined high and low frequency carrier ASSRs at different AM rates (20, 40, 90 Hz) and found that older subjects had reduced ASSR phase-locking at all AM rates and that ASSRs to a low frequency carrier were correlated with speech perception measures. In their study, some of the elderly subjects had some degree of high frequency pure tone behavioral threshold elevation. Both of these studies suggest that in typical aging, a reduction in the ASSR (amplitude/phase locking) is observed primarily with low frequency carriers.

The current study differs from these prior studies of aging and ASSRs in a number of ways. A white noise carrier was chosen instead of a tonal carrier because noise carriers elicit more robust ASSRs that decrease testing time, likely due to the noise activating the entire cochlea (John et al. 2003). We also opted for a white noise carrier because such stimuli are often used in psychoacoustic studies of temporal processing and therefore allow comparisons across different studies. A second difference was the exploration of AM depth as an independent variable rather than using AM rate or other characteristics. A third difference was the use of a continually swept stimulus as opposed to presenting at discrete AM depths. An advantage of such a technique is that finer resolution of neural activity are possible above and below threshold.

Conceivably, the “neural AM depth threshold” could be estimated by determining the AM depth at which the response transitions from being significant (suprathreshold AM depth) to non-significant (subthreshold AM depth). The rationale for this approach is similar to previously reported “sweep” or “zoom” techniques (Linden et al. 1985; Rodriguez et al. 1986; Picton et al. 2007) for intensity threshold estimations. Another reason for choosing a swept AM depth over discrete AM is that this approach allows for a more accurate characterization of the EFR growth function with increases in AM depth. Large steps in discrete AM depths may easily miss subtle differences in function shapes (e.g., linearly increasing versus sigmoidal shapes).

The current study measured physiological AM processing in the auditory system because it could provide an objective measure of behavioral temporal processing ability. We also chose to include elderly adults because deficits in temporal processing with normal aging have been well established (Gordon-Salant & Fitzgibbons 1999). Further, we assessed the ability of physiological data to estimate behavioral thresholds for AM detection since this may be clinically relevant in detecting functional decrements in processing capacity. In summary, the goals of this study were: (1) determine if the swept AM depth approach corresponds to fixed AM depths and is a viable technique to elicit EFRs; (2) relate the EFR AM depth threshold to behavioral AM depth thresholds; (3) examine differences in AM depth thresholds in young NH and older listeners using both the EFR and behavioral responses; (4) compare AM depth-EFR growth functions in young NH and older listeners.

MATERIALS AND METHODS

Subjects

A total of 38 adults (15 females) participated in the study, comprising a YNH group (n=12, aged 18 to 28 years, mean 23 years, 7 females), a first older group (O1; n=12, aged 41 to 63 years, mean 55 years, 4 females) and a second older group with a higher mean age (O2; n=12, aged 67 to 82 years, mean 74 years, 4 females). All YNH individuals had normal pure tone thresholds (less than 20 dB HL) measured at 250, 500, 1000, 2000, and 4000 Hz. This was assessed using ER3A earphones and a GSI 61 Clinical audiometer with a 10 dB down/5 dB up bracketing procedure. Subjects in the O1 and O2 groups had elevated pure tone audiograms, consistent with age-related hearing loss.

The experimental protocols were approved by the Institutional Review Board of the University of California Irvine. Subjects were recruited from the Center for Hearing Research at Irvine database and the University of California Irvine student community. Written informed consent was obtained from each subject after the nature of the study was explained. Subjects were paid to participate in the study.

Stimuli

For all evoked potential stimuli, a wideband noise carrier (using the Matlab function `rand.m`) was amplitude modulated at the fixed rate of 41.0156 Hz. Evoked responses to fixed AM depths were obtained using depths of 100%, 75%, 50% and 25% and consisted of 16 epochs of 1.024-sec each and each recording trial included 30 such sweeps. A swept AM stimulus used modulation depths ranging from 2% to 100% across each stimulus sweep of 40 epochs. Each swept stimulus condition was comprised of three replication trials of 30 sweeps each, and each replication lasted 20.48-mins for a total recording time for swept data of approximately 1 hour. The AM% depth was ramped linearly upward during the first 20.48 seconds of the sweep (20 epochs) and linearly downward over the same range during the second 20 epochs. The rate of change of amplitude modulation depth was 4.785% per second. Sweeps were constructed so that they could be concatenated and repeated without acoustic transients (Purcell et al. 2004). Fixed depth stimuli were recorded for 11 minutes at each depth for depth at 100%, 75%, 50%, and 25% for a total of 44 minutes.

Both fixed and swept EFR stimuli and stimuli for the psychoacoustic AM detection (see below) were presented to the right ear. In some cases where the pure tone threshold was elevated more in the right ear, the left was used. The right ear was used for all 12 of the YNH subjects, 10 out of 12 subjects for the O1 group, and 11 out of 12 subjects for the O2 group. Stimuli were presented at 60 dB SL where 0 dB SL was the threshold intensity for detecting white noise (0% AM depth). The sound pressure level of the 0% AM stimulus was measured using a Brüel and Kjær sound level meter (Investigator 2260) in a 2cc coupler DB0138 set on A weighting with a “slow” time constant. A wideband noise carrier has energy at all frequencies, but when presented through the Etymotic ER3A transducer, energy above 5 kHz is attenuated by more than 10 dB, reaching 30 dB attenuation by 7 kHz.

All 36 subjects were tested in the sweep AM condition, however due to time constraints for some of the subjects, only 24 subjects participated in the fixed AM depth condition (YNH, n=9; O1, n=5; O2, n=10).

Stimulus Presentation and Physiological Response Recording

The experiment was controlled by software developed using LabVIEW (Version 8.5, National Instruments). A National Instruments USB-6221 BNC X-series acquisition system provided digital-to-analog conversion of the stimulus with 16-bit resolution at a rate of 32,000 samples/sec. The level of the stimuli were adjusted by routing the signals through an GSI-61 Clinical audiometer. The sounds were produced using an Etymotic ER3A earphone whose sound tube was sealed in the ear-canal using a disposable foam insert. The EEG was recorded from three gold plated Grass electrodes using GRASS Technologies EC2 electrode cream. Electrodes were located at the vertex (Cz; noninverting) and just below the hairline at the posterior midline of the neck (inverting) with a ground (or common) on the collarbone.

Electrode impedances were assessed using an F-EZM5 GRASS impedance meter and were <5000 ohm at 10 Hz. Inter-electrode differences were <2000 ohm. The three electrode leads were braided and then connected to a GRASS LP511 amplifier that applied a gain of 50,000, and a filter having a pass-band of 0.3 to 300 Hz. The 6221 system applied a further gain of two (for a total gain of 100k) before digitizing the output signal of the GRASS amplifier at 32,000 samples/sec using 16-bit resolution.

Data were collected with subjects residing in a sound-insulated and electromagnetically shielded booth. Subjects reclined in a comfortable chair with a pillow under their neck to help support their head. The lights were on, and they were allowed to watch a muted, closed-captioned movie of their choice. A window was available in order to view the subject to confirm that the subject remained awake. In between recordings, the subject was encouraged to take breaks. The full recording session lasted between 2.5 and 3 hours, including condition 1 (swept AM depth), condition 2 (fixed AM depth), behavioral testing of AM detection, set-up, hearing testing, and breaks.

Physiological Response Analysis

Real-time summary results and indices of EEG signal quality were displayed during data collection to monitor the quality of the recordings and inform if a subject was producing too much EMG activity. A more extensive sweep analysis was then performed off-line using a

custom LabVIEW 8.5 program derived with improvements from previous studies (Purcell et al. 2004; Purcell et al. 2006). In the offline analysis, individual 1.024-sec epochs were automatically rejected by the software from a synchronous average sweep if they did not meet certain criteria. First, a noise metric was calculated for every epoch of a stimulus condition by determining the average amplitude of EEG frequencies in a 20 Hz band spanning the modulation rate of the evoking stimulus (31 to 51 Hz). The mean and standard deviation (SD) of this noise metric was calculated across all epochs. A rejection criterion was then set using the mean +2SD, and all epochs that exceeded this criterion were rejected from the mean response sweep. Additionally, epochs were automatically rejected by the software if any saturation of the amplifier occurred (for example, due to a large myogenic artifact from subject movement) as reflected by points of the recorded EEG waveform having either the maximum or minimum value of the analog to digital converter. This rejection procedure can lead to a different number of epochs contributing to each of the 40 mean epochs that comprise an averaged sweep. If many epochs were rejected, then this might be a cause for concern due to different signal-to-noise ratios (SNRs) for different portions of the averaged sweep. In practice, only 2.5% of epochs were typically rejected, and these were randomly distributed across the averaged sweep. Non-rejected data were synchronously averaged in the time domain to create a mean response sweep (see John et al., 2001).

The ASSRs were measured in the mean sweep data using a software implemented Fourier analyzer ("FA", Regan 1989; Purcell et al. 2004; Purcell et al. 2006). In this method, orthogonal reference sinusoids are matched in frequency to the instantaneous stimulus modulation rate of 41.0156 Hz. An estimated physiological delay of 30 ms was used to improve alignment between the reference and response waveforms during the analysis (Aiken & Picton 2006). This single delay is an estimate of the physiological delays present in an 40 Hz ASSR composed of both cortical and brainstem sources (Purcell et al. 2004; see their Table I "30-50 Hz apparent latency" column where younger and older groups had delays of approximately 25 and 35 ms, respectively). The slow sweeping of AM% depth used here (i.e., 4.785% per sec), likely caused this delay correction to have a very small effect on the estimated response, but it is prudent nonetheless. Two 1.024 sec. rectangular window filters were applied in series to each of the complex outputs of the FA. Because the mean response sweep was evoked by a stimulus with symmetrical increasing and decreasing modulation depths in each half, the second half of the FA output was folded over and vector averaged with the first half. This was done to improve the SNR of the measured responses. A final 512 ms smoothing filter was applied to the amplitude values calculated from the complex FA outputs. To provide a cross-check for the FA results, a discrete Fourier transform (DFT) was also used to estimate the ASSR in the fixed AM% depth condition after similar noise rejection and sweep averaging.

The probability that the estimated ASSR amplitude was drawn from the distribution of the background noise was determined using an F-ratio (Zurek 1992). The characteristics of the background noise were estimated using a DFT calculated from the mean response sweep folded and averaged in the time domain. For the fixed depth conditions, the average noise levels in +/- 60 DFT frequency bins (having 0.122 Hz frequency resolution for a total range of +/-7.32 Hz) were multiplied by a scaling factor of 2.43 (determined using simulated

noise) to compensate for the narrower effective bandwidth of the DFT compared with that of the FA. For the swept depth condition, the average noise levels in +/- 143 DFT bins (having 0.049 Hz frequency resolution for a total range of +/-6.98 Hz) were multiplied by a scaling factor of 3.72. Only the noise estimates were multiplied by these scaling factors, so they could be compared directly with the ASSR amplitudes determined by the FA. The ASSRs were considered significantly different from the background noise estimates when the SNR was ~5 dB. In other words, to reach a $p < 0.05$ level, the amplitude F-ratio evaluated using 2 and 240 degrees of freedom for fixed depth conditions must be above 1.742. For the swept depth condition, there were 2 and 572 degrees of freedom, with a critical value of 1.735 (John & Picton 2000).

Physiological Threshold Estimation

The physiological threshold for detection of amplitude modulation was defined as the smallest modulation depth for which the corresponding ASSR amplitude led to a detectable ASSR with an F-ratio probability value of less than 0.05.

Behavioral Threshold Testing

Behavioral Modulation thresholds were measured using a three-alternative forced choice (3AFC) tracking procedure carried out using a custom built MATLAB testing program. Based upon the subject's preference, one ear was selected to receive the stimuli during the 3AFC test. During each trial of the 3AFC procedure, three sounds are presented sequentially. The sounds were randomly selected to be a wideband noise which was sinusoidally modulated at 41 Hz or two different wideband noises. The observer was required to identify the sound that contained the modulated noise and was provided with feedback from the program which indicated whether the choice was correct. Reversals occurred when a subject incorrectly/correctly responded to two or more consecutive stimuli or vice versa. A large step size (50% change in modulation depth) was used for the first three reversals and then a smaller step size (20% change in modulation depth) was used for the remaining reversals (i.e., an adaptive step size was relied upon). Each run had a total of 12 reversals and the threshold was calculated as the mean of the last eight reversals.

Statistical Analysis

The data were analyzed using repeated measures ANOVA and Pearson correlations. Specific details are described when referred to in the results.

In order to quantify the differences in shape of the EFR as a function of AM depth we modeled individual EFR amplitude versus AM depth results in a customized Matlab sigmoidal function fit using the following formula:

$$EFR\ magnitude = Noise + \frac{A}{(1 + e^{\frac{-(AM\ depth - x_{50})}{B}})}$$

The following parameters were fit for each EFR versus AM depth recording: Noise and A were the upper and lower limits of the function. B determined the degree of linearity of the

function such that with small values of B, the EFR amplitude remains at low amplitude for much of the AM depth range, followed by a sharp increase in amplitude (steep slope) and finally a plateau. With large values of B, the shape of the function resembles a linear function with a shallow slope. The X50 component reflects the AM depth for which the EFR amplitude is 50% of its maximum value. For a sigmoid function, this will cause shifts left and right. Two further measures were derived from the model: the knee point of the AM depth at which the function begins to saturate, and the dynamic range (DR). The DR is the AM % difference between 10% and 90% of the EFR amplitude range. Therefore, if a function was sigmoidal with a steep slope, the AM difference between 10% and 90% of EFR amplitude (DR) would be very small. A shallow function on the other hand would have a large DR.

In addition to the EFR magnitude, the EFR phase was also examined as a function of AM depth. In contrast to the magnitude, phase showed a general decrease with increasing AM depth. The phase vs. AM depth relationship was quantified using a linear regression model in the form of $y=mx+b$ where m equals the slope, y equals the phase, and x equals the AM depth, and b the intercept where the phase at 0 AM depth. Because the phase of EEG noise can vary anywhere from 0 to 360°, only significant EFRs were submitted to the linear regression, and this included AM depths that ranged from 25% to 100%. Mean slopes and intercepts were calculated for each subject in the 3 different groups.

RESULTS

Two of the 38 participants were removed from data analysis. One NH subject requested to be removed from the study before he completed the full testing session and one O2 subject was excluded because of excessive noise due to muscle artifact. In a clinical situation, these subjects would have been re-tested or would have required that the testing session duration be increased (to allow sufficient time to improve SNR through extended averaging). This was not performed in the current study because of time constraints of our subjects.

Behavioral data

An ANOVA showed that the behavioral pure tone thresholds were elevated in the O2 group compared to YNH for 500 Hz [main group effect: $F(2,29)=5.9$; $p=0.007$ and post-hoc YNH vs. O2, $p=0.005$] and for 1000 Hz [main group effect: $F(2,29)=7.0$; $p=0.003$ and posthoc YNH vs. O2, $p=0.002$]. For 2000 Hz, the O2 group had greater thresholds compared to both YNH and O1 groups [main group effect: $(F2,29)=14.0$; $p<0.001$ and posthoc YNH vs. O2, $p=0.001$ and O1 vs. O2, $p=0.012$]. For 4000 Hz, the YNH group, had lower thresholds compared to both O1 and O2, and the O1 and O2 groups did not differ [main group effect: $(F2,29)=17.0$; $p<0.001$ and posthoc YNH vs. O1, $p=0.005$ and YNH vs. O2, $p<0.001$].

Pure tone and AM detection thresholds for all three groups are given in Table 1. Although the mean for AM detection showed that YNH had the lowest AM thresholds, followed by O1, then O2, no significant group differences were observed.

Even though no group differences existed for AM detection, subtle differences may have been obscured by the averaging procedure across set age groups. Therefore we decided to

correlate AM detection with age. Figure 2 shows mean AM detection thresholds for modulated broadband noise across the three groups with individual thresholds plotted as a function of age. No significant correlation was found between age and AM detection thresholds, nor were any significant correlations observed between any of the pure tone thresholds and AM detection results. However, as expected, significant correlations were observed between the pure tone thresholds and age [500 Hz, $r=0.72$; 1000 Hz, $r=0.55$; 2000 Hz, $r=0.65$; 4000 Hz, $r=0.70$; all at $p<0.001$].

Electrophysiology

Sweep EFRs - Amplitude—Significant responses were recorded for all subjects. The general pattern of the EFR amplitude was greater amplitude with larger AM depths. With low AM depths approaching behavioral threshold, the EFR became non-significant. Figure 3 shows a sample subject whose EFR became non-significant at the same AM depth as behavioral threshold. The lowest AM depth for which a significant EFR could be recorded was defined as the EFR threshold (dashed line indicates the noise estimate). In this particular subject, both AM behavioral detection and EFR threshold were 8%. In some instances (10 out of the 39 subjects) there were small regions of non-significant responses (typically spanning a range less than 5% at low AM depths) even though the response was significant again at lower AM depths. These regions of non-significance likely represent instances of an EFR that is near threshold, but may have higher transient noise at these particular times in the recording sweep. Setting the EFR threshold at a higher AM depth, above the regions of non-significance would likely overestimate the threshold EFR depth. We therefore decided to adapt a threshold rule we previously used for estimating ASSR pure tone thresholds (Dimitrijevic et al., 2001) where regions of a response function might show a non-significant value even though there was a significant response at lower intensities. In the current study, if the region of non-significance was less than 5% (17 bins) and the response became significant at a lower AM depth, it needed to remain continuously significant for at least 5% in order to be used in the threshold estimation.

EFRs separately averaged across each of three groups are shown in Figure 4. The YNH subjects appeared to have a relatively linear increase in EFR amplitude while the O2 appeared to have a different shape resembling a sigmoid. Note that there were three O2 subjects who had extremely large EFR amplitudes and mean EFR waveforms were re-plotted excluding these three subjects. The averages of the top five EFR amplitudes (typically elicited by the 95 to 100% AM depth portion of the stimulus) were 400 and 341 nV for YNH and O1, respectively. For O2, the top five amplitude means for all twelve subjects was 491 nV. The three subjects with abnormally large amplitudes, had top five amplitude means of 700, 991 and 1190 nV. Without these three subjects, the mean EFR amplitude was 335 nV, and much closer to the O1 group. It should be noted that we believe these abnormally large EFRs are genuine responses. All three of these subjects were re-tested in a follow up session, and had similar EFR magnitudes to the first session. We also verified that no artifact was present (that might present as erroneously large responses) in the follow up session with occluded insert earphones. With the occluded earphone approach, there is no sound delivered to the ear and therefore no biological responses should be

present. However, we would expect a 5% false positive rate if the EFR/ASSR detection criteria was set to $p < 0.05$.

Averages of the EFR modeled responses across the different groups are shown in Figure 5. The general shape of the EFR amplitude vs. AM depth function resembled a sigmoid. However, the degree of linearity (quantified by the B parameter) appeared to vary among groups, such that YNH and O1 groups appeared more linear and the O2 group appeared to saturate at the maximum EFR amplitude. The mean parameters of the model fits are shown in Figure 6.

A one-way ANOVA was used to examine differences between modeled parameters across the different groups (using all O2 subjects). For the B parameter (linearity) a main effect of group [$F(2,33)=3.5$; $p=0.042$] was observed and posthoc analysis revealed that YNH had a larger B parameter compared to O2 ($p=0.042$). For the X50 parameter, a main effect of group was observed [$F(2,33)=8.4$; $p=0.001$] and posthoc analysis revealed that YNH had a larger X50 parameter compared to O2 ($p=0.006$) and O1 was larger than O2 ($p=0.002$). For DR, a main effect of group was observed [$F(2,33)=4.0$; $p=0.042$] and posthoc analysis revealed that YNH had a larger dynamic range compared to O2 ($p=0.022$). No differences were observed in the A, noise floor, nor knee point parameters.

Given that the three subjects in the O2 group had abnormally large responses, we re-ran comparisons of modeled parameters ANOVAs excluding these three participants. Overall, the effects remained the same except for parameter B such that there was no longer a significant difference between groups ($p=0.07$). The X50 parameter still showed a significant group effect ($F(2,30)=5.9$; $p=0.007$) with posthoc analyses showing that the O2 group had smaller X50's compared to both YNH ($p=0.020$) and O1 ($p=0.009$). The DR still showed a significant group effect [$F(2,30)=3.3$; $p=0.049$] with posthoc analyses showing that the O2 group had a smaller DR compared to YNH ($p=0.040$).

Modeled Parameters Correlations with age—Pearson correlations were performed between each of the fitted parameters and ages of the subject. Significant correlations were observed between: age and B ($r=-0.36$ $p=0.033$), age and X50 ($r=-0.38$ $p=0.020$) and age and DR ($r=-0.39$ $p=0.018$), all shown in Figure 7. No significant relationships with age were observed for A, noise floor, nor knee point parameters.

Relationship between Behavioral AM Detection and EFR amplitude—Mean EFR AM depth thresholds were similar to the behavioral AM detection thresholds (see Table 1): YNH (behavioral: 11.5%, EFR: 9.1%); O1 (behavioral: 14.3%, EFR: 11.9%); O2 (behavioral: 14.9%, EFR: 11.3%). A significant correlation between thresholds for AM behavioral detection and EFR threshold ($r=0.48$ $p=0.003$). Figure 8 shows individual data points and the linear correlation.

Sweep EFRs - Phase—In addition to amplitude, the phase of the EFR was examined. Figure 9 shows the EFR phase for all three experimental groups. The YNH group showed a plateau-like response in phase with varying depth of AM whereas the two older groups both showed a negative slope indicating that phase decreased as a function of AM depth. A one-

way ANOVA indicated a significant group effect for phase slope [$F(2,33)=1.7$; $p=0.045$] and posthoc analysis revealed that the YNH group's phase slope ($-0.05^\circ/\text{AM}\%$) was significantly greater (more flat) than the O2 group (phase slope: $-0.28^\circ/\text{AM}\%$; $p=0.020$). Although the O1 group's phase slope ($-0.24^\circ/\text{AM}\%$) was numerically steeper than the YNH group, this difference failed to reach significance ($p=0.052$). No group differences were observed for the intercept. The three O2 subjects who had abnormally large EFR amplitudes had phases comparable to the other O2 participants.

In order to help understand the functional significance of these phase-slope differences, we assessed the bivariate relationship between phase-slope and age, hearing thresholds, and AM % detection thresholds. Significant bivariate correlations with phase slope were observed for age ($r=-0.37$; $p=0.028$), pure tone threshold at 2 kHz ($r=-0.41$; $p=0.015$), and pure tone threshold at 4 kHz ($r=-0.59$; $p<0.001$). No significant correlations were observed for AM% detection threshold. Age, 2 kHz threshold, and 4 kHz threshold, were entered as predictors of phase-slope difference in a standard multiple linear regression model. We observed a significant overall model $R=0.60$, [$F(2,32)=6.1$; $p=0.002$]. Among the three predictors, only 4 kHz threshold emerged as a significant independent predictor in the model (semipartial correlation = -0.42 ; $p=0.005$).

Sweep EFR versus ASSR at fixed AM depth—To compare whether sweep EFR amplitude values were similar to traditional ASSRs recorded at fixed depths, we extracted the EFR amplitude values corresponding to the same AM depths for which we had “fixed AM depth” ASSR data (100, 75, 50, and 25%). Paired t-tests showed that there were no statistically significant differences were seen between fixed and EFR values. Mean values are shown in Table 2.

Discussion

The results of this study revealed four findings: (1) EFRs to sweep AM depth stimuli can be recorded and provide amplitude measures comparable to ASSRs recorded at fixed AM depths. (2) The minimum AM depth for which an EFR can be elicited is related to behavioral AM detection. (3) Aging does not necessarily affect the overall amplitude of the brain's response to AM stimuli but rather differences are apparent in the relationship between AM depth and EFR, such that the responses were more nonlinear and result in smaller dynamic ranges compared to younger adults. (4) The phase of EFR did not change as a function of AM depth for the young normal hearing controls, but did for the older group.

The EFR technique as a correlate of neural AM depth coding and behavior

The results of the current study showed that sweep EFR amplitudes are remarkably similar to ASSRs recorded at the same fixed AM depth and no significant differences were observed between the two response types (Table 2). Using “sweep” stimuli (termed “zoom” or “ramped” stimuli by others), for which a non-stationary ASSR (i.e., EFR) has been recorded to a “changing” stimulus, has previously been reported for intensity changes (Rodriguez et al. 1986; Linden et al. 1985; Picton et al. 2007) and AM rate changes (Purcell et al. 2004; Poulsen et al. 2009; Poulsen et al. 2007). The present study adds to the current body of

knowledge and demonstrates that non-stationary ASSRs (or EFRs) can also be reliably recorded to varying AM depth. Previous work examining ASSRs at various AM depths have reported linear (Kuwada et al. 1986) or non-linear (Ross et al. 2000; Rees et al. 1986; Picton et al. 1987) relationships. Our data suggests that the degree of linearity varied across the different subject groups, quantified by the B factor where smaller values of the B result in steeper slopes and non-linearity at high modulation depths where the function saturates. In YNH, the EFR-AM depth function had larger B values, indicating a more linear and shallower slope with less saturation compared to the O2 subjects.

In young normal hearing subjects, Picton et al. (1987), used a 1000 Hz carrier tone with 39 Hz AM and found behavioral AM depth thresholds were on average 5% while ASSR depth thresholds were almost the same at 4.9%. We also found very similar thresholds between behavior and EFR: for YNH, behavioral was 11.5% and EFR 9.1%. The overall values of the AM differed from Picton et al., (1987), i.e., near 5% and 10% are likely due to our use of a white noise carrier. A weak ($r=0.48$) but statistically significant ($p=0.003$) correlation was observed between behavioral AM detection and EFR thresholds (see Figure 8). Although noise carriers and tones may produce different results, a likely reason for our low correlation is that there was not sufficient variation in behavioral AM detection thresholds across subjects. The inclusion of patient populations such as auditory neuropathy with known elevated AM detection thresholds (Zeng et al. 2005) would likely strengthen the relationship. The current study has provided both theoretical and practical bases for undertaking such an investigation.

Effects of aging on the EFR

The results of the current study showed that aging does not change the overall amplitude of the EFR but rather affects the shape of the EFR amplitude versus AM depth function. Three parameters (i.e., B, x50, and DR) were shown to be related to aging not only by demonstrating significant group differences (Figure 6) but also significant correlations with age (Figure 7). The “B” parameter and DR are related. B is inversely related to the slope of the sigmoidal function: small values result in a rapid amplitude change to maximum peak values whereas high values show a more gradual change to peak amplitude values. “DR” is a measure of how effectively the auditory system is able to differentiate between different AM depths. For example, a very low DR functionally translates into an “all or none” type of neural encoding of AM depth, whereas a high DR captures the response amplitude changes to varying depths of AM. Reduced X50 in the older O2 group was also observed suggesting that neural populations encoding AM saturate earlier with aging.

It is not clear why the knee point (AM depth for saturation) did not differ between groups. One can speculate how these parameters are related to human hearing and specifically performance in both quiet and noise. Normal speech is composed of varying degrees of AM depth with varying AM rate (Rosen 1992). The addition of noise effectively reduces the depth of AM by filling in the “valleys” in the speech envelope. A reduced neural DR for AM encoding would effectively decrease speech intelligibility by obscuring subtle differences in amplitude fluctuations in speech. This phenomenon may be related to the perceptual

difficulties with speech perception in noise the elderly often report when listening in challenging environments (Pichora-Fuller & Souza 2003).

A recent review by Bharadwaj et al. (2014) posits that “cochlear neuropathy”, also referred to as “hidden hearing loss” is thought to play a role in aging (Plack et al. 2014), through selective loss of low spontaneous rate auditory fibers and leading to impaired speech perception in noise. Bharadwaj suggests that use of ASSRs to AM stimuli of varied depth may reveal differences associated with “cochlear neuropathy” since high spontaneous rate auditory nerve fibers would be saturated, leaving only low spontaneous rate fibers to encode the modulation. These fibers are mostly responsible for suprathreshold coding. The reduced DR we observed with aging is consistent with a reduction in the number of neurons being able to encode intermediate AM depths. One important caveat is that we did not measure speech perception in quiet or noise. Caution is warranted when relating these parameters to speech perception.

A limited number of studies have examined ASSRs as a function of AM depth in older listeners. Leigh-Paffenroth and Fowler (2006) examined 20, 40 and 90 Hz ASSRs to 500 and 2000 Hz tone carriers with various AM depths (10%, 20%, 50%, 80% and 100%) in older subjects (mean age 70 years). The ASSR was quantified using phase locking measures to the modulation. For 40 Hz, older subjects had fewer phased-locked 500 Hz responses compared to younger controls and this reduction was related to speech perception measures. Boettcher et al. (2001) examined, in older adults and young controls, carriers of 520 Hz and 4000 Hz modulated at 40 Hz with AM depths ranging from 5% to 100%. No differences in amplitudes were found between the two groups. Our results are similar to Boettcher et al., (2001) in that no amplitude differences were seen between the older groups and YNH (with the exception of the three subjects with abnormally large responses). Additionally, we found differences the EFR function versus AM depth using our finer resolution AM stimuli. Relating our current findings to Leigh-Paffenroth and Fowler (2006) is difficult because of differences in stimuli and assessment metrics, and we did not assess speech perception.

It remains unclear why some O2 subjects had atypically large EFR amplitudes. The other fitted parameters of their modeled data were in the normal range except for the maximum amplitude. Hearing levels, audiogram shape and AM depth detection thresholds were also in normal ranges for the O2 group. The large amplitudes may be related to common generator of the 40 Hz ASSR and the auditory middle latency response P1 (Bohórquez & Ozdamar 2008). Some previous work has suggested that P1 may be larger with aging (Woods & Clayworth 1986; Alain & McDonald 2007), although this would not account for why the other O2 subjects did not differ from YNH. A follow up study examining the different EFR-AM depth fit parameters to other behavioral measures such as speech perception is warranted.

Phase of EFR

The phase versus AM depth function (phase-slope) was relatively flat in the YNH group but was negative in the older groups (figure 9). Modulation depth versus ASSR functions are much less studied than intensity versus ASSR functions and therefore interpretation of what these functions represent is less straightforward. Intensity functions often show reduced

amplitudes and prolonged latencies with lower level sounds (Picton et al. 2007). The latency (or phase) change with intensity is thought to be related to acceleration of the rise time of the stimulus envelope (Heil 1997). With progressively less AM depth, there would be shallower AM envelopes which would predict longer latencies. However when responses were detectable in the YNH group, phase/latency remained relatively constant. With the older groups, phase/latency decreased with increasing AM depth. There is limited published data on the phase of the 40 Hz ASSR as a function of AM depth and carrier frequency. In YNH subjects, using pure tones ranging from 500 to 4000 Hz, Picton et al. (1987) found very little change in phase as a function of AM depth. Conversely, Ross et al. (2001) found systematic decreases in the ASSR phase as a function of AM depth using MEG recordings for a 250 Hz carrier (40 Hz AM). In animals, little change in phase has been observed in the inferior colliculus with decreasing AM depth (Brugge et al. 1993). In the present study, the underlying reasons for the differences in phase slope versus AM depth between young and older groups is not entirely clear. In the current study, white noise was used as a carrier and therefore there are contributions from both high and low carrier frequency coding neurons that sum together to yield a composite EFR recorded at the scalp. In the older groups, the EFR has a relatively large low frequency carrier component because of their high frequency hearing loss. In fact, the phase-slope with AM depth was significantly related to pure tone thresholds at 4 kHz. This would suggest that the phase slope differences in the older group are driven by low frequency carriers, perhaps at or below 250 Hz given that Ross et al. (2001) observed phase differences with this carrier in YNH listeners. ASSRs to high frequency carriers have an earlier latency compared to low frequency carriers for cortical ASSRs (Stapells et al. 1984; Cohen et al. 1991). If the overall response (from 2% to 100% AM) were dominated equally by high and low carriers, then the entire EFR versus AM depth function would be shifted for the older group compared to YNH. Instead, the divergence between the YNH and older groups occurred at AM depths above ~40% (thus leading to a slope difference). This data therefore suggests that AM coding at high AM depths (above 40%) is impacted substantially by high frequency carriers, whereas low modulation depths elicit normal (young-like) responses when low frequency carriers are dominant. Further studies examining the role between low and high carrier frequency contributions are warranted. Age is not likely driving this effect given that the partial correlation of age was not significant in the multiple linear regression analysis.

Conclusion

The results of the current study reveal the following findings: swept AM depth stimuli can elicit robust responses similar to fixed depth stimuli, the EFR AM depth thresholds were related to behavioral measures of AM depth detection, the shape of the EFR function differed with age with elderly subjects having reduced DRs. The current study has established a solid foundation for the application of the swept AM depth approach to the auditory neuropathy population in which a larger range of AM detection thresholds would be expected.

Acknowledgments

Source of Funding: This research was funded by a grant from the Hearing Foundation of Canada and the National Institutes of Health (P30 DC008369).

References

- Aiken SJ, Picton TW. Envelope and spectral frequency-following responses to vowel sounds. *Hear Res.* 2008; 245:35–47. [PubMed: 18765275]
- Alain C, McDonald KL. Age-related differences in neuromagnetic brain activity underlying concurrent sound perception. *J Neurosci.* 2007; 27:1308–1314. [PubMed: 17287505]
- Anderson S, Parbery-Clark A, White-Schwoch T, et al. Aging affects neural precision of speech encoding. *J Neurosci.* 2012; 32:14156–64. [PubMed: 23055485]
- Bharadwaj H, Verhulst S, Shaheen L, et al. Cochlear neuropathy and the coding of supra-threshold sound. *Front Syst Neurosci.* 2014; 8
- Boettcher FA, Poth EA, Mills JH, et al. The amplitude-modulation following response in young and aged human subjects. *Hear Res.* 2001; 153:32–42. [PubMed: 11223295]
- Bohórquez J, Ozdamar O. Generation of the 40-Hz auditory steady-state response (ASSR) explained using convolution. *Clin Neurophysiol.* 2008; 119:2598–607. [PubMed: 18818122]
- Brugge JF, Blatchley B, Kudoh M. Encoding of amplitude-modulated tones by neurons of the inferior colliculus of the kitten. *Brain Res.* 1993; 615:199–217. [PubMed: 8364731]
- Caspary DM, Hughes LF, Ling LL. Age-related GABAA receptor changes in rat auditory cortex. *Neurobiol Aging.* 2013; 34:1486–96. [PubMed: 23257264]
- Cohen LT, Rickards FW, Clark GM. A comparison of steady-state evoked potentials to modulated tones in awake and sleeping humans. *J Acoust Soc Am.* 1991; 90:2467–2479. [PubMed: 1774415]
- Gordon-Salant S, Fitzgibbons P. Profile of auditory temporal processing in older listeners. *J Speech, Lang* 1999; 42:300–311.
- John MS, Dimitrijevic A, Picton TW. Efficient stimuli for evoking auditory steady-state responses. *Ear Hear.* 2003; 24:406–423. [PubMed: 14534411]
- John MS, Dimitrijevic A, Picton TW. Weighted averaging of steady-state responses. *Clin Neurophysiol.* 2001; 112:555–562. [PubMed: 11222980]
- Kuwada S, Batra R, Maher VL. Scalp potentials of normal and hearing-impaired subjects in response to sinusoidally amplitude-modulated tones. *Hear Res.* 1986; 21:179–192. [PubMed: 3700256]
- Leigh-Paffenroth E, Fowler C. Amplitude-modulated auditory steady-state responses in younger and older listeners. *J Am Acadamey Audiol.* 2006; 17:582–597.
- Linden RD, Campbell KB, Hamel G, et al. Human auditory steady-state evoked potentials during sleep. *Ear Hear.* 1985; 6:167–174. [PubMed: 4007303]
- Pichora-Fuller MK, Schneider Ba, Macdonald E, et al. Temporal jitter disrupts speech intelligibility: a simulation of auditory aging. *Hear Res.* 2007; 223:114–21. [PubMed: 17157462]
- Pichora-Fuller MK, Souza PE. Effects of aging on auditory processing of speech. *Int J Audiol.* 2003; 42(Suppl 2):2S11–S16. [PubMed: 12918623]
- Picton T. Hearing in time: evoked potential studies of temporal processing. *Ear Hear.* 2013; 34:385–401. [PubMed: 24005840]
- Picton TW, van Roon P, John MS. Human auditory steady-state responses during sweeps of intensity. *Ear Hear.* 2007; 28:542–557. [PubMed: 17609615]
- Picton TW, Skinner CR, Champagne SC, et al. Potentials evoked by the sinusoidal modulation of the amplitude or frequency of a tone. *J Acoust Soc Am.* 1987; 82:165–178. [PubMed: 3624637]
- Plack CJ, Barker D, Prendergast G. Perceptual consequences of “hidden” hearing loss. *Trends Hear.* 2014; 18:1–11.
- Poulsen C, Picton TW, Paus T. Age-related changes in transient and oscillatory brain responses to auditory stimulation during early adolescence. *Dev Sci.* 2009; 12:220–35. [PubMed: 19143796]

- Poulsen C, Picton TW, Paus T. Age-related changes in transient and oscillatory brain responses to auditory stimulation in healthy adults 19-45 years old. *Cereb Cortex*. 2007; 17:1454–67. [PubMed: 16916887]
- Purcell DW, John SM, Schneider BA, et al. Human temporal auditory acuity as assessed by envelope following responses. *J Acoust Soc Am*. 2004; 116:3581–3593. [PubMed: 15658709]
- Purcell DW, Van Roon P, John MS, et al. Simultaneous latency estimations for distortion product otoacoustic emissions and envelope following responses. *J Acoust Soc Am*. 2006; 119:2869–80. [PubMed: 16708945]
- Rees A, Green GG, Kay RH. Steady-state evoked responses to sinusoidally amplitude-modulated sounds recorded in man. *Hear Res*. 1986; 23:123–133. [PubMed: 3745015]
- Regan, D. *Human Brain Electrophysiology: Evoked Potentials and Evoked Magnetic Fields in Science and Medicine*. New York: Elsevier Science; 1989.
- Richardson BD, Ling LL, Uteshev VV, et al. Reduced GABA(A) receptor-mediated tonic inhibition in aged rat auditory thalamus. *J Neurosci*. 2013; 33:1218–27a. [PubMed: 23325258]
- Rodriguez R, Picton TW, Linden D, et al. Human auditory steady state responses: effects of intensity and frequency. *Ear Hear*. 1986; 7:300–313. [PubMed: 3770325]
- Rosen S. Temporal information in speech: acoustic, auditory and linguistic aspects. *Philos Trans R Soc Lond B Biol Sci*. 1992; 336:367–73. [PubMed: 1354376]
- Ross B, Borgmann C, Draganova R, et al. A high-precision magnetoencephalographic study of human auditory steady-state responses to amplitude-modulated tones. *J ...* 2000; 2:679–691.
- Shannon RV, Zeng FG, Kamath V, et al. Speech recognition with primarily temporal cues. *Science* (80-.). 1995; 270:303–304.
- Stapells DR, Linden D, Suffield JB, et al. Human auditory steady state potentials. *Ear Hear*. 1984; 5:105–113. [PubMed: 6724170]
- Starr A, Picton TW, Sininger Y, et al. Auditory neuropathy. *Brain*. 1996; 119(Pt 3):741–753. [PubMed: 8673487]
- Takahashi GA, Bacon SP. Modulation detection, modulation masking, and speech understanding in noise in the elderly. *J Speech Hear Res*. 1992; 35:1410–1421. [PubMed: 1494284]
- Viemeister NF. Temporal modulation transfer functions based upon modulation thresholds. *J Acoust Soc Am*. 1979; 66:1364–80. [PubMed: 500975]
- Wang H, Turner JG, Ling L, et al. Age-related changes in glycine receptor subunit composition and binding in dorsal cochlear nucleus. *Neuroscience*. 2009; 160:227–39. [PubMed: 19217931]
- Woods D, Clayworth C. Age-related changes in human middle latency auditory evoked potentials. *Electroencephalogr Clin ...* 1986; 65:297–303.
- Zeng FG, Kong YY, Michalewski HJ, et al. Perceptual consequences of disrupted auditory nerve activity. *J Neurophysiol*. 2005; 93:3050–3063. [PubMed: 15615831]
- Zeng F-G, Liu S. Speech perception in individuals with auditory neuropathy. *J Speech Lang Hear Res*. 2006; 49:367–80. [PubMed: 16671850]

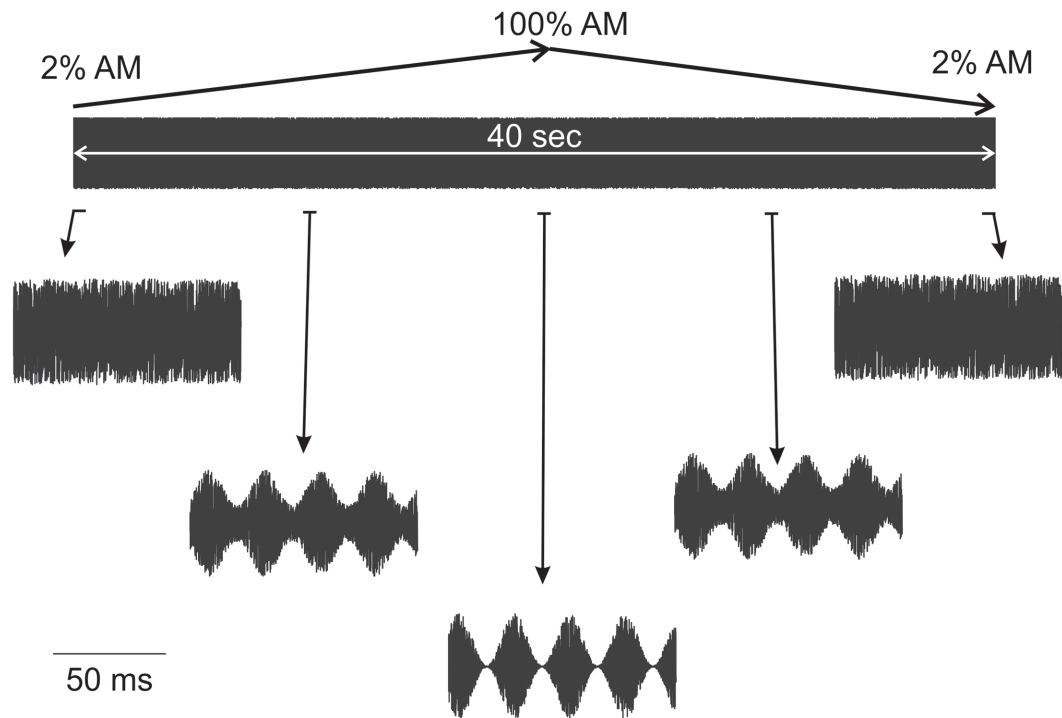


Figure 1.

A 40 second segment of the swept AM depth stimulus is shown. The modulation rate was held constant at 41 Hz while the AM depth varied from 2 to 100% for the first 20 seconds and then 100% to 2% for the last 40 seconds. No transient sounds were heard across successive repetitions of the 40 second sound. Samples of 50 ms are shown to illustrate the AM depth at different time points.

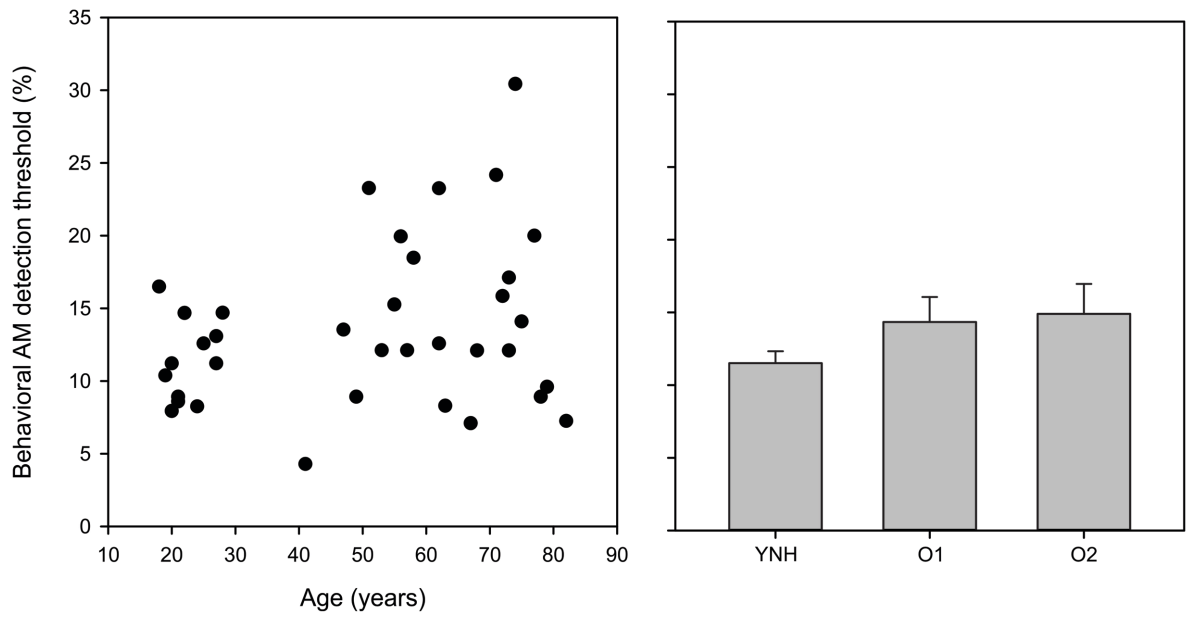


Figure 2.

The left panel shows a scatterplot of the age of the subjects with their corresponding behavioral AM detection thresholds. More variability is seen in AM detection threshold with increasing age, but no systematic increase in AM threshold was seen with age. The right panel shows mean AM detection thresholds for the three groups. Error bars are standard error of the mean.

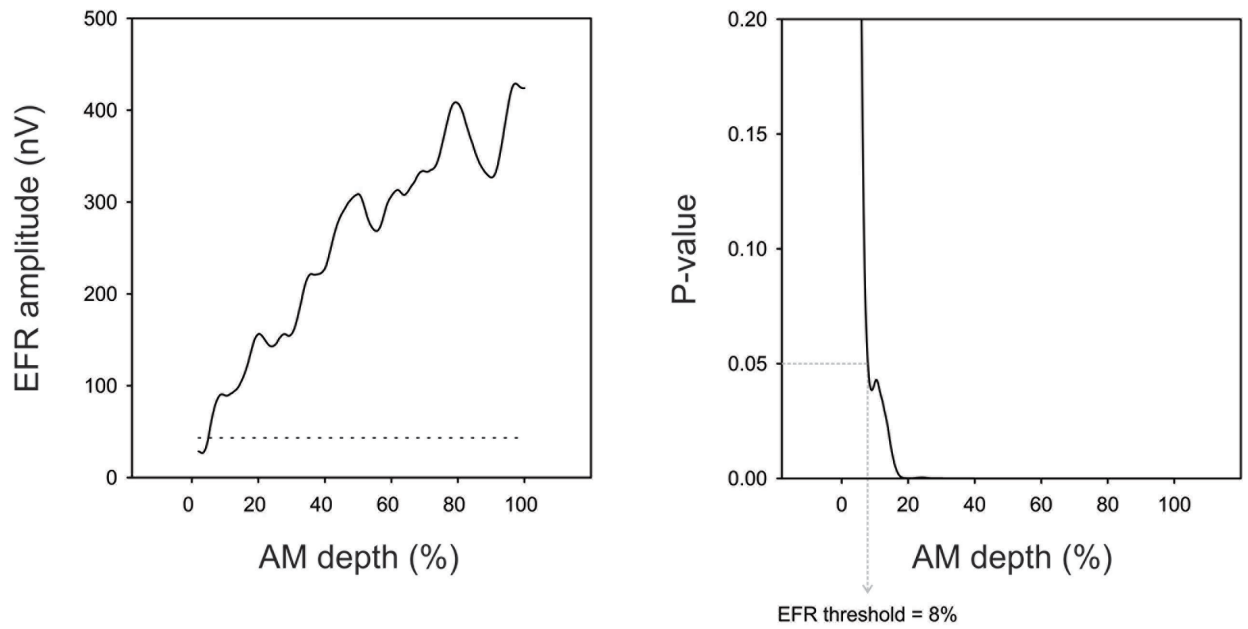
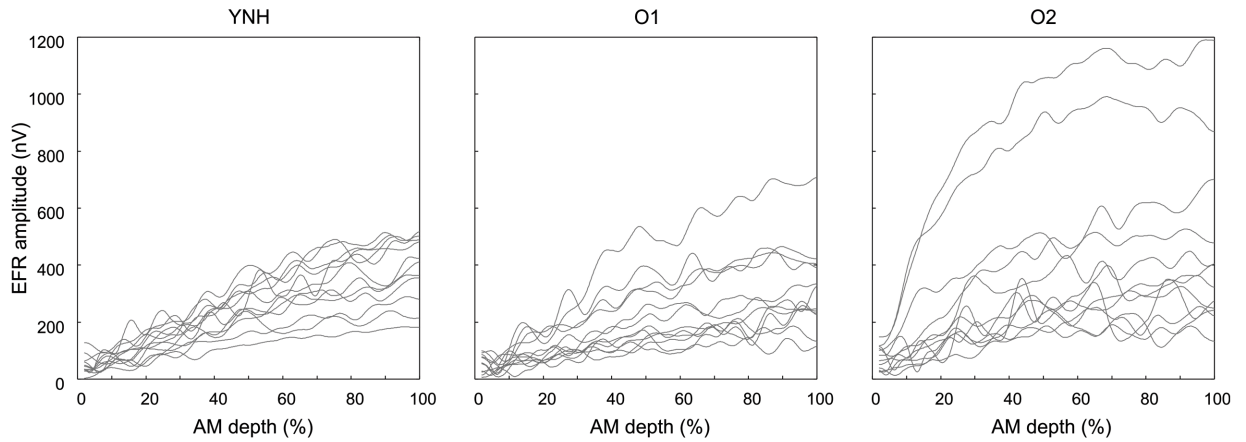


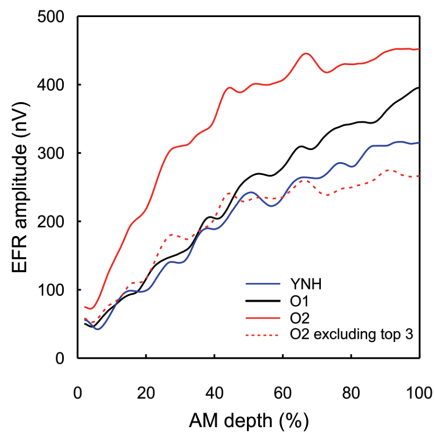
Figure 3.

EFR amplitude (left panel) and P-value (right panel) as a function of AM depth is shown for a sample subject. The noise floor of the EEG recording is shown as a horizontal dashed line on the left panel. Determination of EFR threshold was based on the lowest %AM depth where the EFR was significantly different from the background noise ($p < 0.05$). On the right panel, the dotted line indicates the lowest %AM depth where the EFR was significant ($p = 0.05$). In this case, the EFR threshold was 8%. In this subject, the behavioral threshold for AM detection was also at 8%.

Individual subjects overlaid

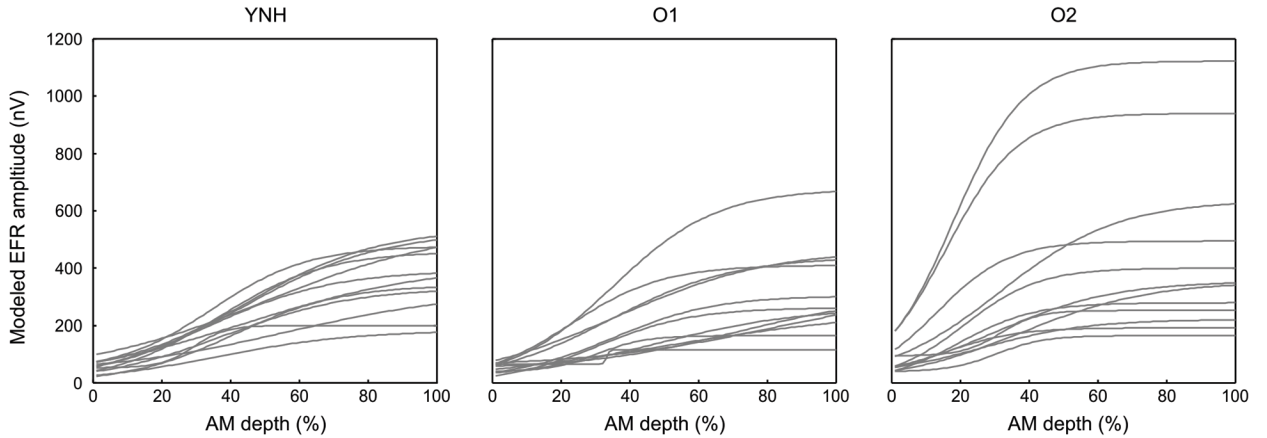


Group mean data

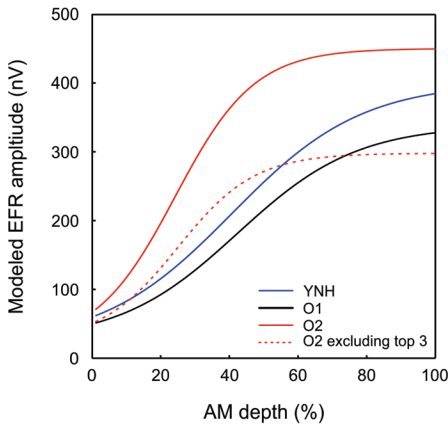
**Figure 4.**

EFR amplitude as a function of %AM depth for all three groups. The top panel shows all subjects overlaid (grey) for the YNH (left), O1 (middle), and O2 (right) groups. The mean group data is shown on the bottom left. The O2 group was subdivided into 2 groups: all subjects $n=12$, solid red and excluding the top 3 subjects showing abnormally large EFRs $n=9$, dashed red.

Individual subjects overlaid



Group mean data



	YNH	O1	O2	O2*
A (max)	380	313	430	273
B (linearity)	19	17	12	11
knee point	44	57	48	52
noise floor	15	20	15	19
dynamic range	59	53	40	39
X50 (%AM for 50% max EFR)	41	42	24	25

* excluding the top 3

Figure 5. Modelled EFR data using the same data as Figure 4. The top panel shows all subjects overlaid (grey) for the YNH (left), O1 (middle), and O2 (right) groups. The mean group data is shown on the bottom left. The bottom right portion of the figure summarizes the parameter values of the model fits across the groups. The A parameter represents the maximum value of the EFR. The B value represents the linearity of the function. With large values, the function is more linear with a shallow slope whereas with small values, the function resembles a sigmoid with a steep slope on the linear portion. The knee point is the AM depth at which the function begins to saturate. The dynamic range is the AM % difference between 10% and 90% of the EFR amplitude range. The X50 is the %AM where EFR is half the maximum amplitude.

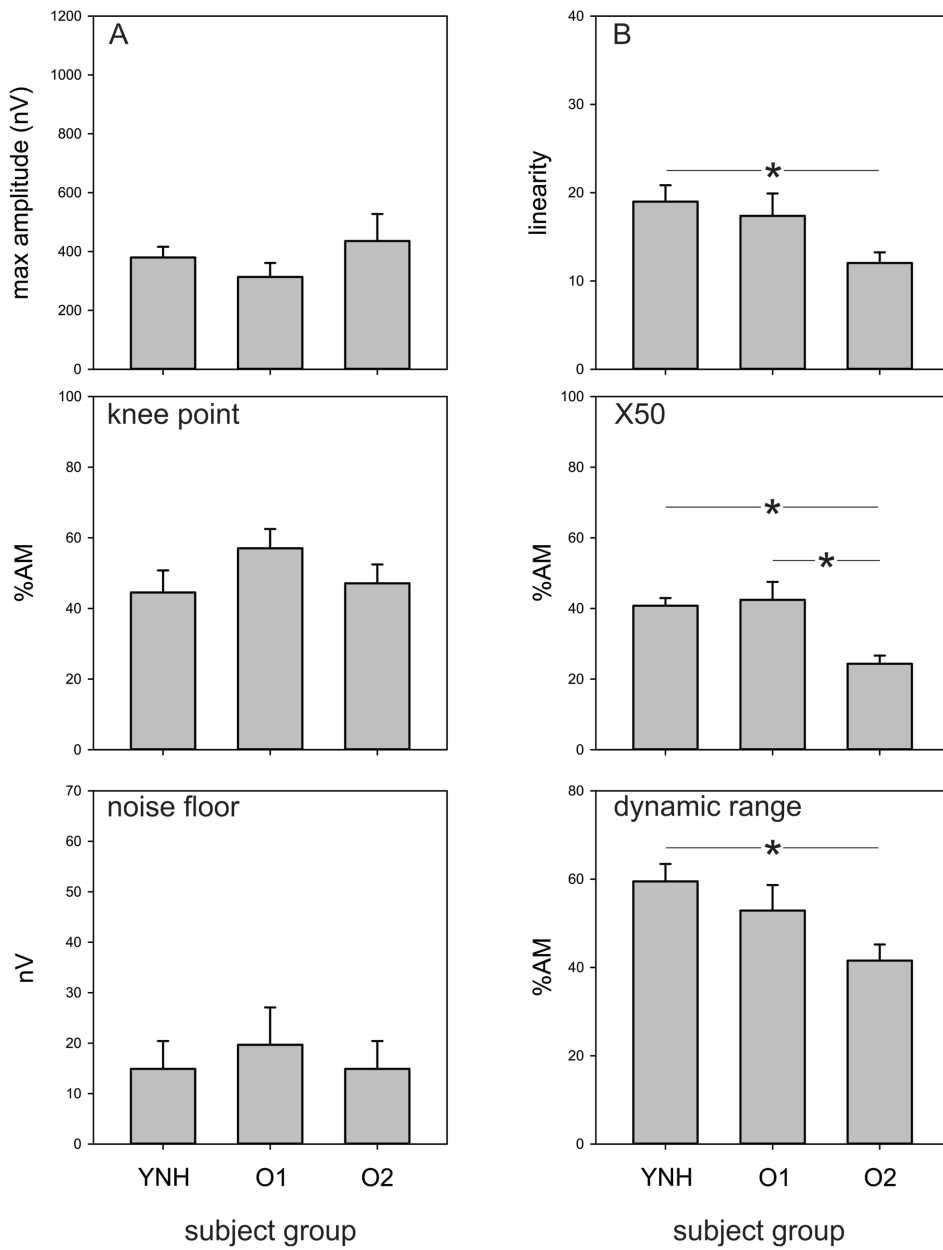


Figure 6. A summary of the modelled parameters of the EFR across the different groups. Error bars are standard error of the mean. Lines with the asterisks represent significantly different comparisons ($p < 0.05$).

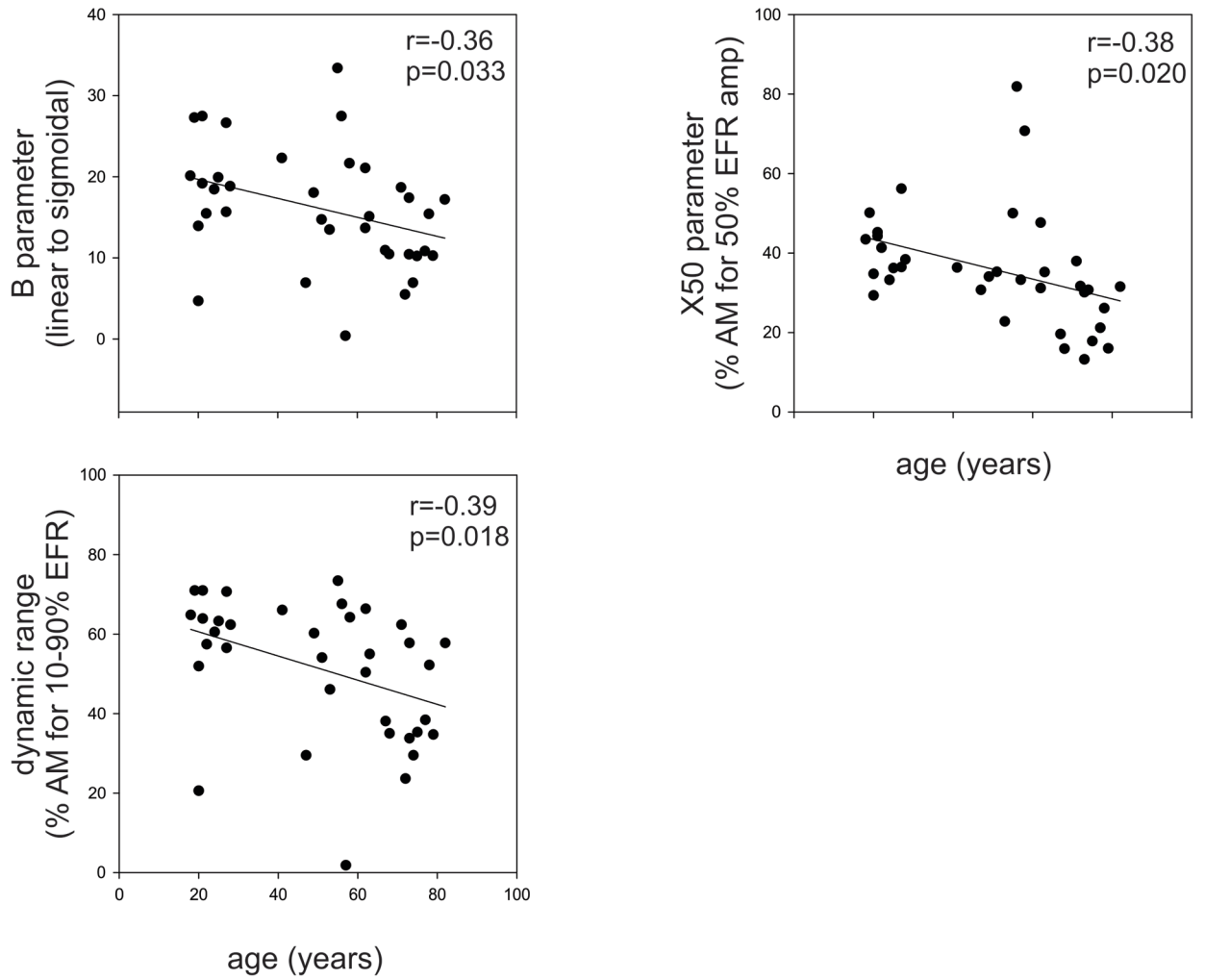


Figure 7. Scatterplots relating the age of subjects to the different modelled parameters. Only significant relationships were plotted.

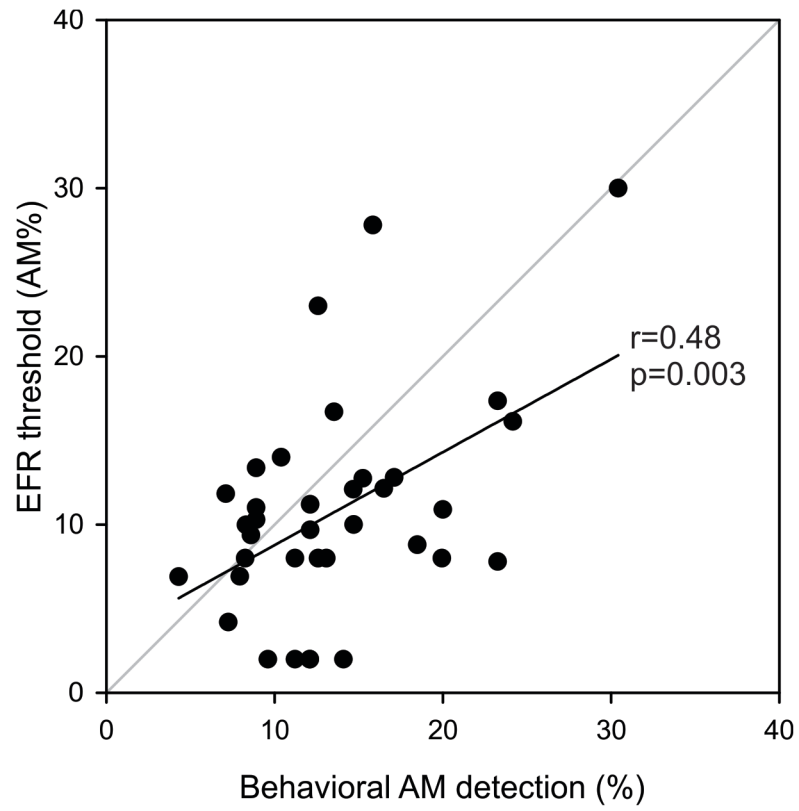


Figure 8. A scatterplot showing a significant correlation between EFR threshold (%AM) and behavioral threshold (%AM).

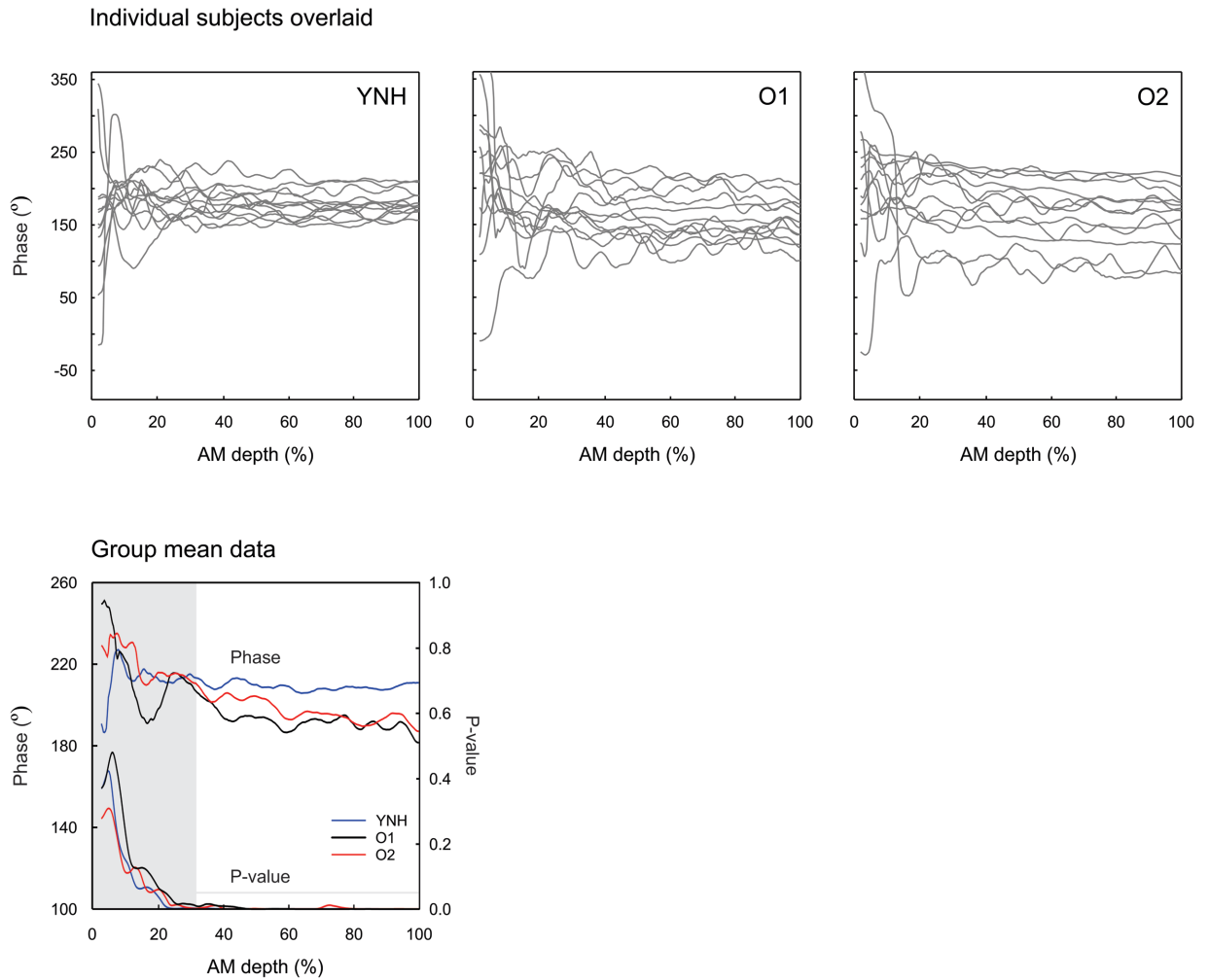


Figure 9.

EFR phase as a function of %AM depth for all three groups. The top panel shows all subjects overlaid (grey) for the YNH (left), O1 (middle), and O2 (right) groups. The mean group data is shown on the bottom left. The group average plot also shows the associated P-values as a function of AM depth. The grey region depicts an AM depth where the responses were significant ($p < 0.05$). The horizontal grey line indicates the $p = 0.05$ level. Note that for YNH subjects, the phase vs. AM depth function is relatively flat whereas for the two older groups, the phase decreases with increased AM depth.

Table 1

Summary of the pure tone audiograms and AM detection thresholds for both behavior and EFR.

Group	Age	Pure tone threshold (dB HL)			AM threshold (%)		Stimulus Intensity (dB SPL)	
		500 Hz	1000 Hz	2000 Hz	4000 Hz	Behavioral		EFR
YNH	22(3)	8(8)	8(5)	5(8)	2(6)	11.5(2.8)	9.1(3.1)	87(7) 70-90
O1	55(7)	19(13)	16(12)	29(15)	29(15)	14.3(5.9)	11.9(4.8)	95(5) 90-105
O2	75(6)	33(20)	35(17)	40(18)	52(28)	14.9(7.1)	11.3(9.8)	104(6) 95-115

Standard deviations are shown in parenthesis. For the last column, stimulus intensity, this was the presentation level for both the AM detection and EFR measures. The last two number indicate the range.

A comparison between sweep EFR amplitudes and fixed AM depth ASSRs are shown. Because the sweep EFR data is continuous, portions of the function corresponding to the same AM depths as the fixed AM depth ASSR were extracted. Note that this data includes the three subjects with high amplitude ASSRs for the O2 group.

Table 2

Group	Sweep EFR (nV) to AM depths				Fixed ASSR (nV) to AM depths			
	100%	75%	50%	25%	100%	75%	50%	25%
YNH	344 (157)	299 (128)	245 (81)	135 (55)	357 (144)	308 (95)	254 (80)	138 (47)
O1	263 (109)	225 (110)	187 (87)	116 (50)	281 (144)	249 (94)	195 (104)	112 (50)
O2	385 (330)	357 (303)	325 (292)	272 (224)	391 (310)	365 (313)	344 (298)	228 (226)

Standard deviations are shown in parenthesis.